

Article

Analytical Decomposition of Transition Flux to Cycle Durations via Integration of Transition Times

Ruizheng Hou 

School of Science, Xi'an University of Technology, Xi'an 710048, China; hourz@xaut.edu.cn

Abstract: Rigorous methods of decomposing kinetic networks to cycles are available, but the solutions usually contain entangled transition rates, which are difficult to analyze. This study proposes a new method of decomposing net transition flux to cycle durations, and the duration of each cycle is an integration of the transition times along the cycle. The method provides a series of neat dependences from the basic kinetic variables to the final flux, which support direct analysis based on the formulas. An assisting transformation diagram from symmetric conductivity to asymmetric conductivity is provided, which largely simplifies the application of the method. The method is likely a useful analytical tool for many studies relevant to kinetics and networks. Applications of the method shall provide new kinetic and thermodynamic information for the studied system.

Keywords: kinetics; network; cycle; transition time; entropy production

1. Introduction

Kinetic networks composed of stochastic transitions between significant states are a useful representation for describing dynamics of complicated systems [1–4]. The representation is broadly used in studying biochemical and biomolecular processes [5–15]. By the representation, the dynamics of a system can be viewed as a combination of different cycles in the network, which not only provides an integrative picture for the dynamics, but also provides a rational way to analyze the dynamics. Rigorous methods [5,6,9,12] for decoupling a network into elementary cycles are available, and fluxes caused by transitions can be decomposed into cycle fluxes by formulas. The methods are useful tools for quantitative studies. Recent single-molecule experiments reveal clear regularities and advances in the thermodynamics and mechanisms of some valuable biomolecular systems [16–22]. For example, the forward vs. backward stepping ratios of the molecular motors kinesin and F_1 -ATPase display clear power law against load [16–18,20], and the load-coupling distances are close to half-step sizes of the motors. The measured energy conversion efficiency of F_0F_1 ATP synthase approaches the thermodynamics limit of 100% [19–22]. The clear regularity and remarkable performance attracted a lot of research effort, and kinetic networks are used for in studies [7]. However, solutions from the present methods [5,6,9,12] usually involve entangled rate constants, in which the rate dependence of the performance and thermodynamics is difficult to analyze directly without numerical assistance. At present, a solution with direct analytical ability is still missing. To find the physical origin of the observed regularities and advances is also difficult. What is missing from the analytical ability is not only about the beauty of the formulation or mathematics, but, and of more relevance, is whether a right angle to see the physics of the systems is found.

The entangled rate constants from the present methods (e.g., refs. [5,6]) likely originate from the type of decomposition. The present methods decompose transition fluxes into cycle fluxes directly, and the cycle fluxes are naturally continuous and inseparable along the cycle. Thus, it is not difficult to understand the appearance of the entangled rate constants in the solution. However, a cycle flux can be alternatively expressed by the reciprocal of the cycle duration, which should be a summation or integration of the durations of



Citation: Hou, R. Analytical Decomposition of Transition Flux to Cycle Durations via Integration of Transition Times. *Symmetry* **2022**, *14*, 1857. <https://doi.org/10.3390/sym14091857>

Academic Editor: Kazuharu Bamba

Received: 11 August 2022

Accepted: 2 September 2022

Published: 6 September 2022

Publisher's Note: MDPI stays neutral with regard to jurisdictional claims in published maps and institutional affiliations.



Copyright: © 2022 by the author. Licensee MDPI, Basel, Switzerland. This article is an open access article distributed under the terms and conditions of the Creative Commons Attribution (CC BY) license (<https://creativecommons.org/licenses/by/4.0/>).

the elementary transitions. Such expression might avoid the entanglement, because basic variables might be separated with each other in the summation. Some effort has been reported on this direction [9]. Thus, the inversed way of expression might provide solutions with analytical ability.

In this study, we propose a general method to decompose steady-state transition flux into cycle durations. The solution contains analytical ability, in which the basic variables are separated with each other, and the dependences from the basic variables to the cycle durations and further to the transition flux are transparent. A general formulation and an assisting transformation diagram approach are provided for the application of the method. In the following sections, we shall firstly demonstrate the method using the minimal case of single cycle for clear understanding, and secondly describe the general formulation. A comparison between this method and a previous method is conducted. Rigorous derivation for supporting the method is shown in the Appendix. Applications of the method are also discussed.

2. Results

2.1. Formulation and Transformation Diagram of Single Cycle

In a transition in a kinetic network, the flux caused by the transition can be understood as contributions from all cycles that pass the transition. In other words, the transition flux can be decomposed into the contributions of the cycles. To clearly display our decomposition, we start from the simplest case of a single cycle. Figure 1A shows a kinetic diagram with a single cycle (1 ↔ 2 ↔ 3 ↔ 4 ↔ 1) composed of four states (marked by 1, 2, 3, and 4) of the system, and transitions (e.g., k_{ij} denotes the transition rate from state i to state j) between the states. For the generality, all the transitions are assumed reversible (e.g., k_{ji} is the reversed rate respect to k_{ij}) (Figure 1A).

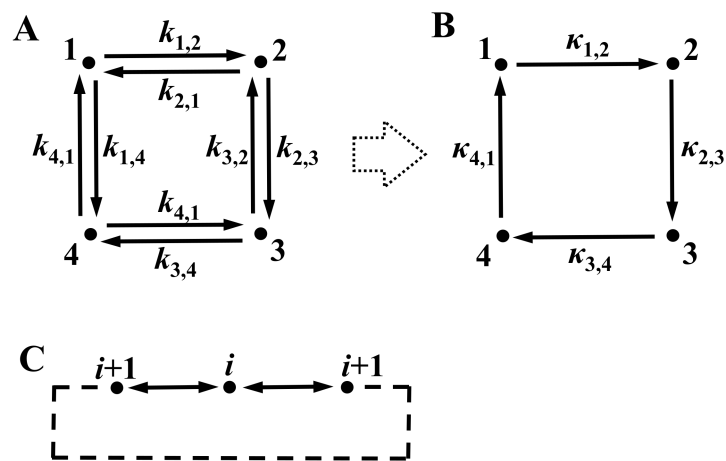


Figure 1. Kinetic diagram of a single cycle. (A) A four-state single cycle is illustrated. Each arrow denotes a transition and the aside k_{ij} denotes the transition rate. (B) Shown is an equivalent diagram of A with the transition rates (k_{ij}) converted to the defined net transition rates (κ_{ij}) (Equation (1)). The cycle, as well as the transitions, now are unidirectional in the form, with the arrows denoting the direction of the net transition and κ_{ij} denoting the net transition rate. κ_{ij} is a composite rate (Equation (1)) that contains the information of both the transition rates (k_{ij} and k_{ji}) in the two opposite directions via the quantity of entropy production (i.e., ΔS_{ij}). (C) Illustration of a single cycle with arbitrary number of states.

Due to the single cycle (Figure 1A), the net transition fluxes (i.e., $J_{ij}^N = p_i k_{ij} - p_j k_{ji}$ with p_i denoting the probability of state i) of all transitions at steady-state equal to each other (e.g., $J_{1,2}^N = J_{2,3}^N = J_{3,4}^N = J_{4,1}^N$ for Figure 1A), and only one cycle (i.e., 1 ↔ 2 ↔ 3 ↔ 4 ↔ 1), contribute to the transition fluxes. For expressing the net transition fluxes by the cycle, we

define the net transition rate from state i to state j as the ratio of the net transition flux over the probability of state i , namely $\kappa_{ij} = J_{ij}^N / p_i$. The net transition rate (κ_{ij}) can be transformed to,

$$\kappa_{ij} = k_{ij}(1 - e^{-\Delta S_{ij}/k_B}) \tag{1}$$

where k_B is the Boltzmann constant, and ΔS_{ij} is the entropy production of a transition from state i to state j , which is defined by $\Delta S_{ij} = k_B \ln((p_i k_{ij}) / (p_j k_{ji}))$ [23,24]. The entropy production ΔS_{ij} can represent irreversibility of the transition. For example, if $e^{\Delta S_{ij}/k_B} \gg 1$ (e.g., $1 - e^{-\Delta S_{ij}/k_B} \geq 0.993$ for $\Delta S_{ij} \geq 5k_B$), κ_{ij} approximates to k_{ij} ($\kappa_{ij} \approx k_{ij}$) (Equation (1)), and, thereby, the reversed rate k_{ji} can be ignored during the calculation of the flux J_{ij}^N . The net flux (J_{ij}^N) of each transition in Figure 1A is expressed by introducing the net transition rate (Appendix A), namely,

$$J_{j,j+1}^N = (\kappa_{1,2}^{-1} + \kappa_{2,3}^{-1} + \kappa_{3,4}^{-1} + \kappa_{4,1}^{-1})^{-1} \tag{2}$$

On the right side of Equation (2), each element of $\kappa_{i,i+1}^{-1}$ is the reciprocal of the net transition rate, and, thereby, $\kappa_{i,i+1}^{-1}$ represents the average time for passing through the transition. The summation of the elements in the bracket is the average duration (τ) of the cycle, namely, $\tau = \kappa_{1,2}^{-1} + \kappa_{2,3}^{-1} + \kappa_{3,4}^{-1} + \kappa_{4,1}^{-1}$. Hence, Equation (2) expresses the net transition flux by the cycle duration via the summation of the transition times, namely, $J_{j,j+1}^N = \tau^{-1}$.

The advantage of Equation (2) is the analytical ability. The expression of net transition flux ($J_{j,j+1}^N$) is simply the reciprocal of cycle duration (τ^{-1}), and the cycle duration is the simple summation of the transition time ($\kappa_{i,i+1}^{-1}$). The relations are clear and understandable. Each transition time ($\kappa_{i,i+1}^{-1}$) appears independently in respect to the others (Equation (2)), and each transition time only depends on the local transition rate ($k_{i,i+1}$) and the local entropy production ($\Delta S_{i,i+1}$) (Equation (1)), which are separated with that of the other transitions. Hence, the series dependences from the basic variables of $k_{i,i+1}$ and $\Delta S_{i,i+1}$ to the intermediate quantities of $\kappa_{i,i+1}$ and τ , and further to the final quantity $J_{j,j+1}^N$, are transparent, which support thorough analysis based on the formulas (Equations (1) and (2)).

Other methods are able to decompose the transition flux too. For example, by exploring the graph theory and kinetics, Hill’s method [5,6] can build complete sets of partial diagrams, directional diagrams, and cycle flux diagrams for the original kinetic diagram. The steady-state probability of each state on the diagram can be expressed by the algebraic values of the directional diagrams, and the flux of a cycle can be expressed by algebraic values of the directional diagrams, as well as by cycle flux diagrams. Thus, the method can simultaneously decompose all the steady-state transition fluxes in a kinetic diagram into cycle fluxes. For comparison with our method, the net flux ($J_{j,j+1}^N$) in Figure 1A is expressed by Hill’s method [5,6], namely,

$$J_{j,j+1}^N = \frac{\chi_+ - \chi_-}{\sigma} \tag{3}$$

$$\chi_+ = k_{1,2}k_{2,3}k_{3,4}k_{4,1} \tag{4}$$

$$\chi_- = k_{1,4}k_{4,3}k_{3,2}k_{2,1} \tag{5}$$

$$\begin{aligned} \sigma = & k_{2,3}k_{3,4}k_{4,1} + k_{4,1}k_{4,3}k_{3,2} + k_{4,1}k_{4,3}k_{2,3} + k_{2,3}k_{3,4}k_{1,4} \\ & + k_{2,1}k_{4,1}k_{3,4} + k_{3,4}k_{4,1}k_{1,2} + k_{2,1}k_{1,4}k_{4,3} + k_{2,1}k_{1,4}k_{3,4} \\ & + k_{3,2}k_{2,1}k_{4,1} + k_{4,1}k_{1,2}k_{3,2} + k_{4,1}k_{1,2}k_{2,3} + k_{3,2}k_{2,1}k_{1,4} \\ & + k_{4,3}k_{3,2}k_{2,1} + k_{1,2}k_{3,2}k_{4,3} + k_{1,2}k_{2,3}k_{4,3} + k_{1,2}k_{2,3}k_{3,4} \end{aligned} \tag{6}$$

In Equations (3)–(6), χ_+ and χ_- are the respective products of the transition rates along the forward and backward directions of the cycle ($1 \leftrightarrow 2 \leftrightarrow 3 \leftrightarrow 4 \leftrightarrow 1$). σ is the sum of algebraic values of directional diagrams, in which each value is a product of the transition rates from the directional diagram. The algebraic value of the cycle flux diagram is unity, which is omitted here. Equation (3) expresses the net transition flux ($J_{j,j+1}^N$) by the cycle

flux, where χ_+/σ and χ_-/σ are the cycle fluxes in the forward and backward directions, respectively, and $(\chi_+ - \chi_-)/\sigma$ is the net cycle flux [5,6]. Equations (3)–(6) use the eight transition rates ($k_{1,2}, k_{2,1}, k_{2,3}, k_{3,2}, k_{3,4}, k_{4,3}, k_{4,1}$, and $k_{1,4}$ in Figure 1A) as basic variables, while Equations (1) and (2) use the four transition rates ($k_{1,2}, k_{2,3}, k_{3,4}$, and $k_{4,1}$) and the four entropy productions ($\Delta S_{1,2}, \Delta S_{2,3}, \Delta S_{3,4}$, and $\Delta S_{4,1}$) as basic variables. As the total number of basic variables are conserved, the two expressions (Equations (2) and (3)) are mathematically equivalent. However, the dependences from the basic variables of the eight transition rates (k_{ij} in Figure 1A) to the final quantities of the net cycle flux $((\chi_+ - \chi_-)/\sigma)$, as well as the net transition flux ($J_{j,j+1}^N$), are complicated, largely due to the transition rates being entangled with each other in the expression (Equations (4)–(6)). Since Figure 1A is a simple single-cycle diagram with only four transitions, the above dependences would be more complicated [5,6] for diagrams containing more cycles.

The reason for the neat expression of Equation (2) is explained by Figure 1B. The rate entanglement in Equations (3)–(6) is more or less due to the reversibility of the transitions in Figure 1A. If all the transitions (Figure 1A) are irreversible, the entanglement will disappear. Our formulation actually creates an equivalent diagram (Figure 1B) to the original one (Figure 1A) with all the transitions converted to a unidirectional form (Figure 1B). The transformation is conducted by using the net transition rates (κ_{ij}) instead of the original transition rates (k_{ij} and k_{ji}) (Figure 1B). The new diagram (Figure 1B) maintains all the kinetic information of the original one (Figure 1A) via the net transition rates (κ_{ij}), because κ_{ij} absorbs the information of the reversed transition via the entropy production (ΔS_{ij}) (Equation (1)). The conductivity of the new diagram is asymmetric compared to the original, which largely simplifies the expression of the net transition flux. The transformation diagram is general, which applies to more complicated kinetic networks. The generality are shown in the later sections.

The simplification from the transformation diagram might be understood as a algebraic transformation from transition rates (k_{ij} and k_{ji}) to entropy production (ΔS_{ij}), while the entropy production is not merely the mathematical transformation but an important physical quantity that is independent. The independence of the entropy production is discussed in the later section of Discussion.

After the four-state single cycle (Figure 1A), a general formula for a single cycle with arbitrary number of states (Figure 1C) can be given (Appendix A), namely,

$$J_{j,j+1}^N = \left(\sum_i \kappa_{i,i+1}^{-1} \right)^{-1} \tag{7}$$

where $J_{j,j+1}^N$ denotes a net transition flux from state j to state $j+1$ in Figure 1C. Similar to Equation (2), Equation (7) also expresses the net transition flux by the duration (τ) of the cycle, namely, $\tau = \sum_i \kappa_{i,i+1}^{-1}$, and the duration is also a summation of the transition time ($\kappa_{i,i+1}^{-1}$). The steady-state condition for the single cycle (Figure 1C) is expressed by Equation (8) or Equation (7), namely,

$$\kappa_{i,i+1} + \kappa_{i,i-1} = 0 \tag{8}$$

$$p_{i-1}\kappa_{i-1,i} + p_{i+1}\kappa_{i+1,i} = 0 \tag{9}$$

Equation (8) indicates the total of the net transition rates from state i is zero, and Equation (9) indicates the total of the net transition fluxes to state i is zero. Equations (8) and (9) are necessary for analysis of the kinetics. For example, our formulation assigns a direction for the net transition flux (also the cycle flux) in Equations (2) ($1 \rightarrow 2$ in Figure 1A) and (7) ($i \rightarrow i + 1$ in Figure 1C), which may not be the actual direction of the flux. Equations (8) and (9) show that the formulas (Equations (2) and (7)) produce negative values if the preassigned direction is opposite to the actual direction.

2.2. Case Analysis for Multiple-Cycle Network

A kinetic network in general can contain multiple cycles. Given a transition of interest, the net transition flux is contributed from the cycles that pass through the transition. In this section, we use a minimal diagram (Figure 2) to show that the above formulation applies to the general case.

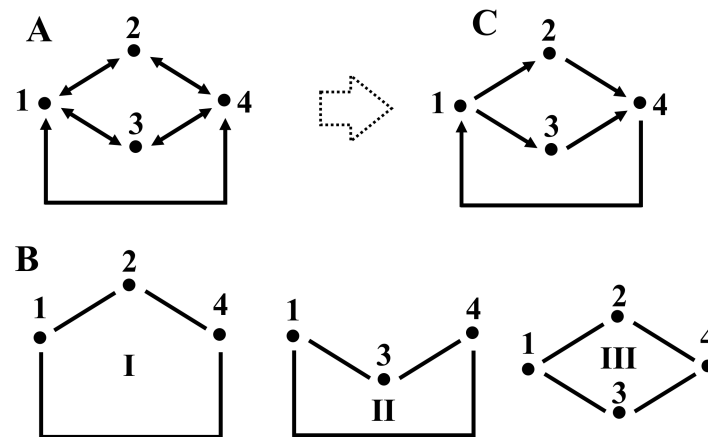


Figure 2. Minimal diagram for multiple cycles. (A) Shown is a minimal kinetic diagram that contains multiple cycles. All the transitions between two states are reversible, which are denoted by the arrows. (B) Shown are the three cycles contained in the diagram of A. The arrows for the transition direction are omitted. (C) Shown is the diagram transformed from A. The transformation is similar to that of Figure 1A to Figure 1B. In the present diagram, all transitions are unidirectional in the form, and each transition is described by the defined net transition rates (κ_{ij}) (Equation (1)) instead of the original transition rates (k_{ij}).

Figure 2A is a minimal diagram that contains three possible cycles, which are shown in Figure 2B (cycle I, II, and III). If the transition $4 \leftrightarrow 1$ is of interest, the net transition flux ($J_{4,1}^N$) should be contributed by the cycle I ($1 \leftrightarrow 2 \leftrightarrow 4 \leftrightarrow 1$) and cycle II ($1 \leftrightarrow 3 \leftrightarrow 4 \leftrightarrow 1$) (Figure 2B). The flux is expressed by the cycles (Appendix B), namely,

$$J_{4,1}^N = \left\{ \frac{\kappa_{1,2}}{\kappa_{1,2} + \kappa_{1,3}} \left((\kappa_{1,2} + \kappa_{1,3})^{-1} + \kappa_{2,4}^{-1} + \kappa_{4,1}^{-1} \right) + \frac{\kappa_{1,3}}{\kappa_{1,2} + \kappa_{1,3}} \left((\kappa_{1,2} + \kappa_{1,3})^{-1} + \kappa_{3,4}^{-1} + \kappa_{4,1}^{-1} \right) \right\}^{-1} \quad (10)$$

In Equation (10), the factors of $\kappa_{1,2}/(\kappa_{1,2} + \kappa_{1,3})$ and $\kappa_{1,3}/(\kappa_{1,2} + \kappa_{1,3})$ are the respective probabilities of the system working in cycle I and cycle II when the transition $4 \leftrightarrow 1$ occurs. As $\kappa_{1,2}$ and $\kappa_{1,3}$ are the respective net transition rates to the two pathways of $1 \rightarrow 2$ and $1 \rightarrow 3$, the probabilities satisfy the flux distribution towards the two pathways at the branching state (state 1). The rest factors of $(\kappa_{1,2} + \kappa_{1,3})^{-1} + \kappa_{2,4}^{-1} + \kappa_{4,1}^{-1}$ and $(\kappa_{1,2} + \kappa_{1,3})^{-1} + \kappa_{3,4}^{-1} + \kappa_{4,1}^{-1}$ are the respective durations of cycle I and II, which are relevant to the transition $4 \leftrightarrow 1$. Here, $(\kappa_{1,2} + \kappa_{1,3})^{-1}$ is the transition time for both transitions of $1 \rightarrow 2$ and $1 \rightarrow 3$, which is different from that of a single cycle (e.g., the transition time is $\kappa_{1,2}^{-1}$ for the transition $1 \rightarrow 2$ in Figure 1A). The difference is caused by the competition between the two transitions ($1 \rightarrow 2$ and $1 \rightarrow 3$) at the branching state (state 1), in which situation only the quicker transition in the stochastic processes occurs and the actual transition times of both transitions are reduced (Appendix). Hence, the net transition flux $J_{4,1}^N$ can be understood as the reciprocal of the average duration of the cycles (I and II) that pass through the transition $4 \leftrightarrow 1$ (Equation (10)).

The formulation also applies to other transitions in Figure 2A. Take transition $2 \leftrightarrow 4$ for example, the net transition flux ($J_{2,4}^N$) is contributed by cycles I and III, which can be expressed (Appendix B) as,

$$J_{2,4}^N = \left\{ \frac{\kappa_{4,1}}{\kappa_{4,1} + \kappa_{4,3}} \left((\kappa_{4,1} + \kappa_{4,3})^{-1} + \kappa_{1,2}^{-1} + \kappa_{2,4}^{-1} \right) + \frac{\kappa_{4,3}}{\kappa_{4,1} + \kappa_{4,3}} \left((\kappa_{4,1} + \kappa_{4,3})^{-1} + \kappa_{3,1}^{-1} + \kappa_{1,2}^{-1} + \kappa_{2,4}^{-1} \right) \right\}^{-1} \quad (11)$$

It is not difficult to find that $J_{2,4}^N$ is still the reciprocal of the average duration of cycle I and cycle III (Equation (11)). The factors of $\kappa_{4,1}/(\kappa_{4,1} + \kappa_{4,3})$ and $\kappa_{4,3}/(\kappa_{4,1} + \kappa_{4,3})$ are the respective probabilities of the system working in cycle I and cycle III, and the rest factors of $(\kappa_{4,1} + \kappa_{4,3})^{-1} + \kappa_{1,2}^{-1} + \kappa_{2,4}^{-1}$ and $(\kappa_{4,1} + \kappa_{4,3})^{-1} + \kappa_{3,1}^{-1} + \kappa_{1,2}^{-1} + \kappa_{2,4}^{-1}$ are the respective durations of cycle I and cycle III.

Equations (10) and (11) show that a net transition flux from a multiple-cycle diagram can still be decomposed into durations of the cycles that pass through the transition, and the durations are still the summations of the transition times. The expressions (Equations (10) and (11)) also contain the same analytical ability of Equations (2) and (7), since the dependences of the final quantity (J_{ij}^N) on the intermediate quantities (cycle probabilities and durations), and further on the basic variables (k_{ij} and ΔS_{ij}) (Equation (1)), remain clear.

The formulation of Equations (10) and (11) still follows the logic of the diagram transformation from Figure 1A to Figure 1B. For example, if the transition $4 \leftrightarrow 1$ (Figure 2A) is of interest, a direction for the net transition flux can be assigned, e.g., $4 \rightarrow 1$, and cycle I and cycle II can be transformed to unidirectional cycles along the direction, namely $1 \rightarrow 2 \rightarrow 4 \rightarrow 1$ for cycle I and $1 \rightarrow 3 \rightarrow 4 \rightarrow 1$ for cycle II. Finally, a new diagram (Figure 2C) is ready with all transition rates (e.g., k_{ij} and k_{ji}) replaced by net transition rates (e.g., κ_{ij}) (similar to Figure 1B). A similar approach applies to transition $2 \leftrightarrow 4$ (Figure 2A) too. The results suggest that a general formulation for the decomposition in an arbitrary network can be given. The formulation is shown in the next section.

2.3. General Formulation for Kinetic Network

In a kinetic network with all transitions reversible, the net flux of a transition from state l_1 to state l_2 can be decomposed into the contributions from the cycles that pass through the transition, namely,

$$J_{l_1 l_2}^N = \left(\sum_{\substack{m = I, II \dots \\ l_1 l_2 \subset C_m}} \rho_m \tau_m \right)^{-1} \tag{12}$$

$$\rho_m = \prod_{ij; ij \subset C_m} \frac{\kappa_{ij}}{\kappa_{ij} + \sum_{n; n \notin C_m} \kappa_{in}} \tag{13}$$

$$\tau_m = \sum_{ij; ij \subset C_m} \left(\kappa_{ij} + \sum_{n; n \notin C_m} \kappa_{in} \right)^{-1} \tag{14}$$

In Equations (12)–(14), m is a number (e.g., I, II, III . . .) assigned to each cycle, and ρ_m and τ_m are the probability and duration, respectively, of cycle m , which contributes to the transition $l_1 \leftrightarrow l_2$. The expression of “ $l_1 l_2 \subset C_m$ ” denotes that the transition $l_1 \leftrightarrow l_2$ is in cycle m , and the expression of “ $n \notin C_m$ ” denotes that the state n is not in cycle m . We need to note that ρ_m and τ_m depend on the transition (e.g., $l_1 \leftrightarrow l_2$) that is decomposed. This is because the calculation of the probability ρ_m (Equation (13)) and duration τ_m (Equation (14)) depends on the set of cycles, which, in turn, depends on the decomposed transition. The steady-state condition for an arbitrary kinetic network can be expressed as,

$$\sum_j \kappa_{ij} = 0 \tag{15}$$

$$\sum_j p_j \kappa_{ji} = 0 \tag{16}$$

The meanings of Equations (15) and (16) are the same of Equations (8) and (9).

Equations (12)–(14) combined with Equation (1) provide an analytical form for decomposing a net transition flux. In a network with n transitions, Equations (12)–(14) contain n net transition rates (i.e., κ_{ij}), which, in turn, depend on n transition rates (i.e., k_{ij}) and

n entropy productions (i.e., ΔS_{ij}) (Equation (1)). Thus, the total number of variables ($2n$) for Equations (12)–(14) is the same as the total number of transition rates. The net transition flux is still the reciprocal of the average cycle duration (Equation (12)). Here, the cycle probability is the product of all the branching probabilities along the cycle (Equation (13)), and the cycle duration is the summation of the transition times (Equation (14)). Thus, the dependences of the final quantities (Equation (12)) on the intermediate quantities (Equation (13), and further on the basic variables (Equation (1)), are clear. The formulation (Equations (12)–(14)) applies to any transition in a given kinetic network at steady state.

Equations (12)–(14) are derived from the transformation diagram similar to that of Figure 1A to Figure 1B, as well as from Figure 2A to Figure 2C. For verification of Equations (12)–(14), five kinetic networks with different connectivity are used (Figure 3). For each diagram (Figure 3), the decomposition based on the transformation diagram (Equations (12)–(14)) is listed in Table 1. For example, the transition $8 \leftrightarrow 1$ in Figure 3A is contributed from the three cycles of $1 \leftrightarrow 2 \leftrightarrow 5 \leftrightarrow 8 \leftrightarrow 1$, $1 \leftrightarrow 3 \leftrightarrow 6 \leftrightarrow 8 \leftrightarrow 1$, and $1 \leftrightarrow 4 \leftrightarrow 7 \leftrightarrow 8 \leftrightarrow 1$. When the transition $8 \leftrightarrow 1$ occurs, the probability of the system working in the first cycle depends on the branching at state 1 (Figure 3A), which is $\kappa_{1,2}/(\kappa_{1,2} + \kappa_{1,3} + \kappa_{1,4})$ (Equation (13)). The duration of the first cycle is the summation of the transition times, namely, $(\kappa_{1,2} + \kappa_{1,3} + \kappa_{1,4})^{-1} + \kappa_{2,5}^{-1} + \kappa_{5,8}^{-1} + \kappa_{8,1}^{-1}$ (Equation (14)). Here, the transition time of $1 \leftrightarrow 2$ ($(\kappa_{1,2} + \kappa_{1,3} + \kappa_{1,4})^{-1}$) is shortened by the branching at state 1 (Figure 3A), which follows Equation (14). Thus, the contribution of the first cycle, as well as the other two cycles, can be derived from the procedure, and the final expression of the net flux ($J_{8,1}^N$) can be given (Table 1) (Equation (12)).

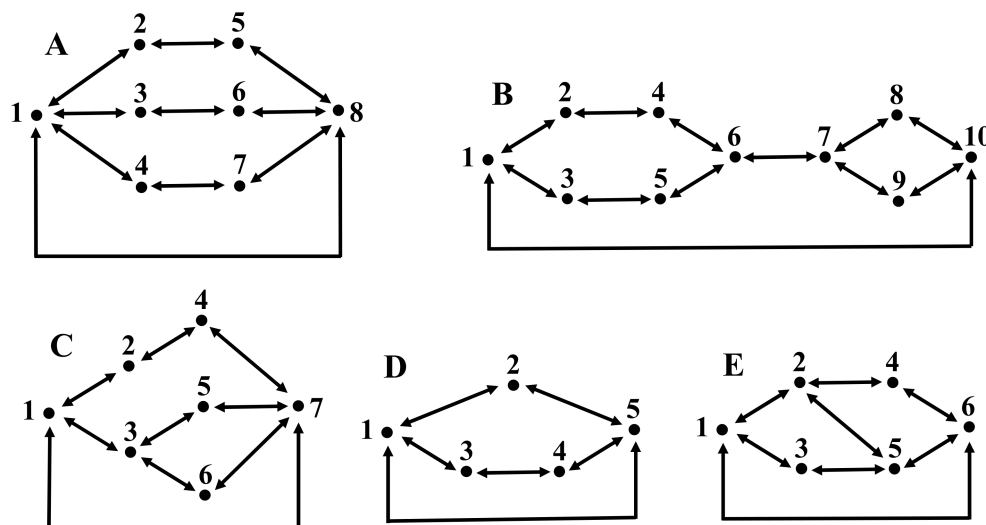


Figure 3. Examples of kinetic networks. Shown are five kinetic networks with different types of connectivity. (A) Shown diagram contains multiple pathways at the branching state (state 1). (B) Shown diagram displays a branching–converging–branching style. (C) Shown diagram contains secondary branching (the branching at state 3 succeeds the branching at state 1). (D) The two pathways ($1 \leftrightarrow 2 \leftrightarrow 5$ and $1 \leftrightarrow 3 \leftrightarrow 4 \leftrightarrow 5$) in the diagram contain different number of states. (E) Shown diagram contains bridge ($2 \leftrightarrow 5$) between two pathways ($1 \leftrightarrow 2 \leftrightarrow 4 \leftrightarrow 6$ and $1 \leftrightarrow 3 \leftrightarrow 5 \leftrightarrow 6$).

For verification, rigorous derivation of the decomposition is shown in the Appendix. The results from the transformation diagram (Table 1) are exactly the same as that from the rigorous derivation (Appendix C). The consistency shows that the diagram transformation (e.g., from Figure 1A to Figure 1B and from Figure 2A to Figure 2C) combined with the rate transformation (i.e., from the transition rate k_{ij} and k_{ji} to the net transition rate κ_{ij} via Equation (1)) (Figure 1B) is a general method for the decomposition. The transformation diagram largely simplifies the application of Equations (12)–(14) because a diagram (or network) of unidirectional transitions is easy to calculate.

Table 1. Examples of net transition flux decomposition. The first column lists the transition and diagram, which are decomposed. The second column lists the cycles that contribute to the transition. The third column lists the probability (ρ_m) of the system working in the cycle when the decomposed transition occurs. The last column lists the duration (τ_m) of the cycle. The results are derived from the transformation diagram, which is equivalent to Equations (13) and (14). The expression of the net transition flux ($J_{i,j}^N$) is ready with the elements of ρ_m and τ_m (Equation (12)).

Flux	Cycle	ρ_m	τ_m
$J_{8,1}^N$ for $8 \leftrightarrow 1$ of Figure 3A	$1 \leftrightarrow 2 \leftrightarrow 5 \leftrightarrow 8 \leftrightarrow 1$	$\frac{\kappa_{1,2}}{\kappa_{1,2} + \kappa_{1,3} + \kappa_{1,4}}$	$(\kappa_{1,2} + \kappa_{1,3} + \kappa_{1,4})^{-1} + \kappa_{2,5}^{-1} + \kappa_{5,8}^{-1} + \kappa_{8,1}^{-1}$
	$1 \leftrightarrow 3 \leftrightarrow 6 \leftrightarrow 8 \leftrightarrow 1$	$\frac{\kappa_{1,3}}{\kappa_{1,2} + \kappa_{1,3} + \kappa_{1,4}}$	$(\kappa_{1,2} + \kappa_{1,3} + \kappa_{1,4})^{-1} + \kappa_{3,6}^{-1} + \kappa_{6,8}^{-1} + \kappa_{8,1}^{-1}$
	$1 \leftrightarrow 4 \leftrightarrow 7 \leftrightarrow 8 \leftrightarrow 1$	$\frac{\kappa_{1,4}}{\kappa_{1,2} + \kappa_{1,3} + \kappa_{1,4}}$	$(\kappa_{1,2} + \kappa_{1,3} + \kappa_{1,4})^{-1} + \kappa_{4,7}^{-1} + \kappa_{7,8}^{-1} + \kappa_{8,1}^{-1}$
$J_{10,1}^N$ for $10 \leftrightarrow 1$ of Figure 3B	$1 \leftrightarrow 2 \leftrightarrow 4 \leftrightarrow 6 \leftrightarrow 7 \leftrightarrow 8 \leftrightarrow 10 \leftrightarrow 1$	$\frac{\kappa_{1,2}}{\kappa_{1,2} + \kappa_{1,3}} \cdot \frac{\kappa_{7,8}}{\kappa_{7,8} + \kappa_{7,9}}$	$(\kappa_{1,2} + \kappa_{1,3})^{-1} + \kappa_{2,4}^{-1} + \kappa_{4,6}^{-1} + \kappa_{6,7}^{-1} + (\kappa_{7,8} + \kappa_{7,9})^{-1} + \kappa_{8,10}^{-1} + \kappa_{10,1}^{-1}$
	$1 \leftrightarrow 2 \leftrightarrow 4 \leftrightarrow 6 \leftrightarrow 7 \leftrightarrow 9 \leftrightarrow 10 \leftrightarrow 1$	$\frac{\kappa_{1,2}}{\kappa_{1,2} + \kappa_{1,3}} \cdot \frac{\kappa_{7,9}}{\kappa_{7,8} + \kappa_{7,9}}$	$(\kappa_{1,2} + \kappa_{1,3})^{-1} + \kappa_{2,4}^{-1} + \kappa_{4,6}^{-1} + \kappa_{6,7}^{-1} + (\kappa_{7,8} + \kappa_{7,9})^{-1} + \kappa_{9,10}^{-1} + \kappa_{10,1}^{-1}$
	$1 \leftrightarrow 3 \leftrightarrow 5 \leftrightarrow 6 \leftrightarrow 7 \leftrightarrow 8 \leftrightarrow 10 \leftrightarrow 1$	$\frac{\kappa_{1,3}}{\kappa_{1,2} + \kappa_{1,3}} \cdot \frac{\kappa_{7,8}}{\kappa_{7,8} + \kappa_{7,9}}$	$(\kappa_{1,2} + \kappa_{1,3})^{-1} + \kappa_{3,5}^{-1} + \kappa_{5,6}^{-1} + \kappa_{6,7}^{-1} + (\kappa_{7,8} + \kappa_{7,9})^{-1} + \kappa_{8,10}^{-1} + \kappa_{10,1}^{-1}$
	$1 \leftrightarrow 3 \leftrightarrow 5 \leftrightarrow 6 \leftrightarrow 7 \leftrightarrow 9 \leftrightarrow 10 \leftrightarrow 1$	$\frac{\kappa_{1,3}}{\kappa_{1,2} + \kappa_{1,3}} \cdot \frac{\kappa_{7,9}}{\kappa_{7,8} + \kappa_{7,9}}$	$(\kappa_{1,2} + \kappa_{1,3})^{-1} + \kappa_{3,5}^{-1} + \kappa_{5,6}^{-1} + \kappa_{6,7}^{-1} + (\kappa_{7,8} + \kappa_{7,9})^{-1} + \kappa_{9,10}^{-1} + \kappa_{10,1}^{-1}$
$J_{7,1}^N$ for $7 \leftrightarrow 1$ of Figure 3C	$1 \leftrightarrow 2 \leftrightarrow 4 \leftrightarrow 7 \leftrightarrow 1$	$\frac{\kappa_{1,2}}{\kappa_{1,2} + \kappa_{1,3}}$	$(\kappa_{1,2} + \kappa_{1,3})^{-1} + \kappa_{2,4}^{-1} + \kappa_{4,7}^{-1} + \kappa_{7,1}^{-1}$
	$1 \leftrightarrow 3 \leftrightarrow 5 \leftrightarrow 7 \leftrightarrow 1$	$\frac{\kappa_{1,3}}{\kappa_{1,2} + \kappa_{1,3}} \cdot \frac{\kappa_{3,5}}{\kappa_{3,5} + \kappa_{3,6}}$	$(\kappa_{1,2} + \kappa_{1,3})^{-1} + (\kappa_{3,5} + \kappa_{3,6})^{-1} + \kappa_{5,7}^{-1} + \kappa_{7,1}^{-1}$
	$1 \leftrightarrow 2 \leftrightarrow 6 \leftrightarrow 7 \leftrightarrow 1$	$\frac{\kappa_{1,3}}{\kappa_{1,2} + \kappa_{1,3}} \cdot \frac{\kappa_{3,6}}{\kappa_{3,5} + \kappa_{3,6}}$	$(\kappa_{1,2} + \kappa_{1,3})^{-1} + (\kappa_{3,5} + \kappa_{3,6})^{-1} + \kappa_{6,7}^{-1} + \kappa_{7,1}^{-1}$
$J_{5,1}^N$ for $5 \leftrightarrow 1$ for Figure 3	$1 \leftrightarrow 2 \leftrightarrow 5 \leftrightarrow 1$	$\frac{\kappa_{1,2}}{\kappa_{1,2} + \kappa_{1,3}}$	$(\kappa_{1,2} + \kappa_{1,3})^{-1} + \kappa_{2,5}^{-1} + \kappa_{5,1}^{-1}$
	$1 \leftrightarrow 3 \leftrightarrow 4 \leftrightarrow 5 \leftrightarrow 1$	$\frac{\kappa_{1,3}}{\kappa_{1,2} + \kappa_{1,3}}$	$(\kappa_{1,2} + \kappa_{1,3})^{-1} + \kappa_{3,4}^{-1} + \kappa_{4,5}^{-1} + \kappa_{5,1}^{-1}$
$J_{6,1}^N$ for $6 \leftrightarrow 1$ of Figure 3E	$1 \leftrightarrow 2 \leftrightarrow 4 \leftrightarrow 6 \leftrightarrow 1$	$\frac{\kappa_{1,2}}{\kappa_{1,2} + \kappa_{1,3}} \cdot \frac{\kappa_{2,4}}{\kappa_{2,4} + \kappa_{2,5}}$	$(\kappa_{1,2} + \kappa_{1,3})^{-1} + (\kappa_{2,4} + \kappa_{2,5})^{-1} + \kappa_{4,6}^{-1} + \kappa_{6,1}^{-1}$
	$1 \leftrightarrow 2 \leftrightarrow 5 \leftrightarrow 6 \leftrightarrow 1$	$\frac{\kappa_{1,2}}{\kappa_{1,2} + \kappa_{1,3}} \cdot \frac{\kappa_{2,5}}{\kappa_{2,4} + \kappa_{2,5}}$	$(\kappa_{1,2} + \kappa_{1,3})^{-1} + (\kappa_{2,4} + \kappa_{2,5})^{-1} + \kappa_{5,6}^{-1} + \kappa_{6,1}^{-1}$
	$1 \leftrightarrow 3 \leftrightarrow 5 \leftrightarrow 6 \leftrightarrow 1$	$\frac{\kappa_{1,3}}{\kappa_{1,2} + \kappa_{1,3}}$	$(\kappa_{1,2} + \kappa_{1,3})^{-1} + \kappa_{3,5}^{-1} + \kappa_{5,6}^{-1} + \kappa_{6,1}^{-1}$

3. Discussions

In general, if a net transition flux is analyzed in the view of the cycles, the transition flux is affected by both of the cycle probabilities (ρ_m) and durations (τ_m) (Equations (12)–(14)). The net transition flux mainly depends on the cycles that contribute the most significant portions of $\rho_m \tau_m$ (Equation (12)). However, a dominance can occur in two different situations; namely, a cycle may dominant via the overwhelming probability (ρ_m) or the super slow duration (τ_m). The dominance by ρ_m requires quicker net transition rates at the branching states for the dominant cycle than the other cycles (Equation (13)), while the dominance by τ_m requires slow net transition rates along the dominant cycle (Equation (14)), as long as the rates generate no diminishing ρ_m at the branching states. The first situation is not difficult to see, while the second situation might be ignored easily. Usually a cycle with a long duration would be judged as a slow cycle of slow transition rates, and thereby, has a small probability of occurring. It is unlikely that such a cycle significantly contributes to the net transition flux. However, the rigorous formulation in this study suggests a slow cycle can contribute most significantly to the net transition flux, as long as the slow transitions (i.e., small net transition rates) do not appear at the branching states.

The definition of net transition rate (Equation (1)) from this study can be used to quantify the actual speed of a transition. The expression (Equation (1)) provides some general information on the driving energy and environmental temperature dependence of the speed. In

Equation (1), the entropy production (ΔS_{ij}) multiplied by the temperature (T) is a measure of driving energy of the transition, namely, $\Delta G_{ij} = T\Delta S_{ij}$ [25]. For general cases, if the driving energy is increased without affecting the other conditions, both the transition rate (k_{ij}) and the entropy production (ΔS_{ij}) increase with the driving energy, and, thereby, the actual speed of transition should increase monotonically with the driving energy (Equation (1)), and the duration of a cycle (Equation (14)) is reduced by the driving energy. In the other case of temperature (T) increase, the transition rate (k_{ij}) is raised by the temperature in general cases, while the other factor of $1 - e^{-\Delta G_{ij}/kBT}$ (Equation (1)) decreases with the temperature, as the thermal energy brought by the increase in temperature reduces the irreversibility of a processes in general. Thus, the temperature dependence of the net transition rate is governed by the two opposite factors, and the rate can be raised or depressed by the temperature. Due to the two opposite factors, a maximum speed or minimal duration of a cycle can be formed at a specific temperature.

The advantage of the presented method is the analytical transparency. By the method, any dependence of a transition time (Equation (1)), cycle probability (Equation (13)), or duration (Equation (14)) on a transition rate (i.e., k_{ij}) or entropy production (i.e., ΔS_{ij}) is easy to be analyzed. Usually, a kinetic network (with n reversible transitions) is accustomed to being analyzed by all the given transition rates ($2n$ rates). In this situation, the entropy productions used in our method still need to be obtained by solving the probabilities of all states (i.e., p_i) via other methods (e.g., Hill's method [5,6]), which seems ease the analysis slightly. However, the aim of our method is to use the half transition rates (n rates) and the entropy productions (n entropy productions) as independent variables, instead of treating the entropy productions as assisting transformations from the basic transition rates. The treatment is applicable. The basic variables of our method contain all the information of the kinetics. One can find that the compound quantity of the net transition rate (κ_{ij}) contains the information for both directions of the transition via the entropy production (Equation (1)), and, thereby, the set of variables of the method is a complete set for representing a network. The entropy production is an independent physical quantity that contains important physical implications [23,24,26–31]. Thus, the quantity can be treated as an independent variable in the method. Applications that use entropy productions as independent quantities are reported for both biosystems [25,32,33] and artificial systems [34,35], which provide useful thermodynamic information for characterizing the systems. Application of the method is likely to reveal new kinetic or thermodynamic information for systems being studied.

4. Conclusions

In summary, a method for decomposing net transition flux into contributions of cycles is presented. The net transition flux is expressed by the reciprocal of the average duration of the cycles that passes through the transition, and the duration of each cycle is a summation of the transition times along the cycle. The method is rigorous and general. The advantage of the method is the analytical ability, which provides neat dependences of quantities of interest on basic variables. The general formulation (Equations (12)–(14)), as well as the general transformation diagram approach (Figure 1A,B), are provided for the application of the method. The method is likely to be a useful tool for many studies on kinetics and networks. As the method uses the thermodynamic quantity of entropy production as a basic variable, the application of the method to specific problems will likely provide new thermodynamic information for the systems.

Funding: This research was funded by National Natural Science Foundation of China under grant No. 11904278, and by the Department of Science and Technology of Shaanxi Province under grant No. 2020JQ-612.

Institutional Review Board Statement: Not applicable.

Informed Consent Statement: Not applicable.

Data Availability Statement: Not applicable.

Conflicts of Interest: The author declares no conflict of interest.

Appendix A. Decomposition for Single Cycle

Given a single cycle at steady-state (e.g., Figure 1C), the net transition fluxes of all transitions along the cycle are equal, namely, $J_{i,i+1}^N = p_i k_{i,i+1} - p_{i+1} k_{i+1,i} = p_j k_{j,j+1} - p_{j+1} k_{j+1,j} = J_{j,j+1}^N$. The steady-state conditions of Equations (8) and (9) are derived from introducing the definition of entropy production ($\Delta S_{ij} = k_B \ln((p_i k_{ij}) / (p_j k_{ji}))$) to the above equality.

By introducing the relation of $p_i k_{i,i+1} - p_{i+1} k_{i+1,i} = p_i \kappa_{i,i+1}$ and the normalization condition of $\sum_i p_i = 1$ to the net transition flux $J_{i,i+1}^N = p_i k_{i,i+1} - p_{i+1} k_{i+1,i}$, Equation (A1) can be given, namely,

$$J_{j,j+1}^N = \left(\frac{\sum_i p_i}{p_j \kappa_{j,j+1}} \right)^{-1} = \left(\sum_i \frac{p_i}{p_i \kappa_{i,i+1}} \right)^{-1} = \left(\sum_i \kappa_{i,i+1}^{-1} \right)^{-1} \tag{A1}$$

Equation (A1) is the same as Equation (7). Application of Equation (A1) to the cycle shown in Figure 1A produces Equation (2).

Appendix B. Decomposition for the Networks

In this part, we illustrate the rigorous derivation of Equations (10) and (11) (for Figure 2A), as well as the results shown in Table 1 (for Figure 3).

Transition 4 ↔ 1 in Figure 2A. Similar to Equation (A1), the net transition flux $J_{4,1}^N$ can be expressed as,

$$J_{4,1}^N = \left(\frac{p_1}{p_1(\kappa_{1,2} + \kappa_{1,3})} + \frac{p_2 + p_3}{p_2 \kappa_{2,4} + p_3 \kappa_{3,4}} + \frac{p_4}{p_4 \kappa_{4,1}} \right)^{-1} = \left(\frac{1}{\kappa_{1,2} + \kappa_{1,3}} + \frac{1}{\kappa_{2,4} + \frac{p_3}{p_2} \kappa_{3,4}} + \frac{1}{\frac{p_2}{p_3} \kappa_{2,4} + \kappa_{3,4}} + \frac{1}{\kappa_{4,1}} \right)^{-1} \tag{A2}$$

Application of the steady-state condition (Equations (15) and (16)) on states 2 and 3 (Figure 2A) produces the ratios between the probabilities in Equation (A2), namely $p_2/p_1 = \kappa_{1,2}/\kappa_{2,4}$, $p_3/p_1 = \kappa_{1,3}/\kappa_{3,4}$, and $p_2/p_3 = (\kappa_{1,2}\kappa_{3,4})/(\kappa_{1,3}\kappa_{2,4})$. Equation (A2) is simplified by replacing the ratios, namely,

$$J_{4,1}^N = \left\{ \frac{\kappa_{1,2}}{\kappa_{1,2} + \kappa_{1,3}} \left(\frac{1}{\kappa_{1,2} + \kappa_{1,3}} + \frac{1}{\kappa_{2,4}} + \frac{1}{\kappa_{4,1}} \right) + \frac{\kappa_{1,3}}{\kappa_{1,2} + \kappa_{1,3}} \left(\frac{1}{\kappa_{1,2} + \kappa_{1,3}} + \frac{1}{\kappa_{3,4}} + \frac{1}{\kappa_{4,1}} \right) \right\}^{-1} \tag{A3}$$

Transition 2 ↔ 4 in Figure 2A. Similar to Equation (A2), the net transition flux $J_{2,4}^N$ can be expressed as,

$$J_{2,4}^N = \left(\frac{1}{\kappa_{4,1} + \kappa_{4,3}} + \frac{1}{\kappa_{3,1} + \frac{p_4}{p_3} \kappa_{4,1}} + \frac{1}{\kappa_{1,2}} + \frac{1}{\kappa_{2,4}} \right)^{-1} \tag{A4}$$

Application of Equations (15) and (16) to states 3 and 4 (Figure 2A) generates the ratio of $p_4/p_3 = \kappa_{3,1}/\kappa_{4,3}$. Equation (A4) is simplified by replacing the ratio, namely,

$$J_{2,4}^N = \left\{ \frac{\kappa_{4,1}}{\kappa_{4,1} + \kappa_{4,3}} \left(\frac{1}{\kappa_{4,1} + \kappa_{4,3}} + \frac{1}{\kappa_{1,2}} + \frac{1}{\kappa_{2,4}} \right) + \frac{\kappa_{4,3}}{\kappa_{4,1} + \kappa_{4,3}} \left(\frac{1}{\kappa_{4,1} + \kappa_{4,3}} + \frac{1}{\kappa_{3,1}} + \frac{1}{\kappa_{1,2}} + \frac{1}{\kappa_{2,4}} \right) \right\}^{-1} \tag{A5}$$

Transition 8 ↔ 1 in Figure 3A. Similar to Equation (A2), the net transition flux $J_{8,1}^N$ can be expressed as,

$$J_{8,1}^N = \left(\frac{1}{\kappa_{1,2} + \kappa_{1,3} + \kappa_{1,4}} + \frac{1}{\kappa_{2,5} + \frac{p_3}{p_2} \kappa_{3,6} + \frac{p_4}{p_2} \kappa_{4,7}} + \frac{1}{\frac{p_2}{p_3} \kappa_{2,5} + \kappa_{3,6} + \frac{p_4}{p_3} \kappa_{4,7}} + \frac{1}{\frac{p_2}{p_4} \kappa_{2,5} + \frac{p_3}{p_4} \kappa_{3,6} + \kappa_{4,7}} \right. \tag{A6}$$

$$\left. + \frac{1}{\kappa_{5,8} + \frac{p_6}{p_5} \kappa_{6,8} + \frac{p_7}{p_5} \kappa_{7,8}} + \frac{1}{\frac{p_5}{p_6} \kappa_{5,8} + \kappa_{6,8} + \frac{p_7}{p_6} \kappa_{7,8}} + \frac{1}{\frac{p_5}{p_7} \kappa_{5,8} + \frac{p_6}{p_7} \kappa_{6,8} + \kappa_{7,8}} + \frac{1}{\kappa_{8,1}} \right)^{-1}$$

Application of Equations (15) and (16) to states 2, 3, 4, 5, 6, and 7 (Figure 3A) generates the ratios of $p_2/p_3 = (\kappa_{1,2}\kappa_{3,6})/(\kappa_{1,3}\kappa_{2,5})$, $p_3/p_4 = (\kappa_{1,3}\kappa_{4,7})/(\kappa_{1,4}\kappa_{3,6})$, $p_2/p_4 = (\kappa_{1,2}\kappa_{4,7})/(\kappa_{1,4}\kappa_{2,5})$, $p_5/p_6 = (\kappa_{1,2}\kappa_{6,8})/(\kappa_{1,3}\kappa_{5,8})$, $p_6/p_7 = (\kappa_{1,3}\kappa_{7,8})/(\kappa_{1,4}\kappa_{6,8})$, and $p_5/p_7 = (\kappa_{1,2}\kappa_{7,8})/(\kappa_{1,4}\kappa_{5,8})$. Equation (A6) is simplified by replacing the ratios, namely,

$$J_{8,1}^N = \left\{ \frac{\kappa_{1,2}}{\kappa_{1,2} + \kappa_{1,3} + \kappa_{1,4}} \left(\frac{1}{\kappa_{1,2} + \kappa_{1,3} + \kappa_{1,4}} + \frac{1}{\kappa_{2,5}} + \frac{1}{\kappa_{5,8}} + \frac{1}{\kappa_{8,1}} \right) + \frac{\kappa_{1,3}}{\kappa_{1,2} + \kappa_{1,3} + \kappa_{1,4}} \left(\frac{1}{\kappa_{1,2} + \kappa_{1,3} + \kappa_{1,4}} + \frac{1}{\kappa_{3,6}} + \frac{1}{\kappa_{6,8}} + \frac{1}{\kappa_{8,1}} \right) + \frac{\kappa_{1,4}}{\kappa_{1,2} + \kappa_{1,3} + \kappa_{1,4}} \left(\frac{1}{\kappa_{1,2} + \kappa_{1,3} + \kappa_{1,4}} + \frac{1}{\kappa_{4,7}} + \frac{1}{\kappa_{7,8}} + \frac{1}{\kappa_{8,1}} \right) \right\}^{-1} \tag{A7}$$

Transition 10 ↔ 1 in Figure 3B. Similar to Equation (A2), the net transition flux $J_{10,1}^N$ can be expressed as,

$$J_{10,1}^N = \left(\frac{1}{\kappa_{1,2} + \kappa_{1,3}} + \frac{1}{\kappa_{2,4} + \frac{p_3}{p_2} \kappa_{3,5}} + \frac{p_2}{p_3} \frac{1}{\kappa_{2,4} + \kappa_{3,5}} + \frac{1}{\kappa_{4,6} + \frac{p_5}{p_4} \kappa_{5,6}} + \frac{p_4}{p_5} \frac{1}{\kappa_{4,6} + \kappa_{5,6}} + \frac{1}{\kappa_{6,7}} + \frac{1}{\kappa_{7,8} + \kappa_{7,9}} + \frac{1}{\kappa_{8,10} + \frac{p_9}{p_8} \kappa_{9,10}} + \frac{p_8}{p_9} \frac{1}{\kappa_{8,10} + \kappa_{9,10}} + \frac{1}{\kappa_{10,1}} \right)^{-1} \tag{A8}$$

Application of Equations (15) and (16) to states 2, 3, 4, 5, 8, and 9 generates the ratios of $p_2/p_3 = (\kappa_{1,2}\kappa_{3,5})/(\kappa_{1,3}\kappa_{2,4})$, $p_4/p_5 = (\kappa_{1,2}\kappa_{5,6})/(\kappa_{1,3}\kappa_{4,6})$, and $p_8/p_9 = (\kappa_{7,8}\kappa_{9,10})/(\kappa_{7,9}\kappa_{8,10})$. Equation (A8) can be transformed by replacing the ratios, namely,

$$J_{10,1}^N = \left\{ \frac{\kappa_{1,2}}{\kappa_{1,2} + \kappa_{1,3}} \frac{\kappa_{7,8}}{\kappa_{7,8} + \kappa_{7,9}} \left(\frac{1}{\kappa_{1,2} + \kappa_{1,3}} + \frac{1}{\kappa_{2,4}} + \frac{1}{\kappa_{4,6}} + \frac{1}{\kappa_{6,7}} + \frac{1}{\kappa_{7,8} + \kappa_{7,9}} + \frac{1}{\kappa_{8,10}} + \frac{1}{\kappa_{10,1}} \right) + \frac{\kappa_{1,2}}{\kappa_{1,2} + \kappa_{1,3}} \frac{\kappa_{7,9}}{\kappa_{7,8} + \kappa_{7,9}} \left(\frac{1}{\kappa_{1,2} + \kappa_{1,3}} + \frac{1}{\kappa_{2,4}} + \frac{1}{\kappa_{4,6}} + \frac{1}{\kappa_{6,7}} + \frac{1}{\kappa_{7,8} + \kappa_{7,9}} + \frac{1}{\kappa_{9,10}} + \frac{1}{\kappa_{10,1}} \right) + \frac{\kappa_{1,3}}{\kappa_{1,2} + \kappa_{1,3}} \frac{\kappa_{7,8}}{\kappa_{7,8} + \kappa_{7,9}} \left(\frac{1}{\kappa_{1,2} + \kappa_{1,3}} + \frac{1}{\kappa_{3,5}} + \frac{1}{\kappa_{5,6}} + \frac{1}{\kappa_{6,7}} + \frac{1}{\kappa_{7,8} + \kappa_{7,9}} + \frac{1}{\kappa_{8,10}} + \frac{1}{\kappa_{10,1}} \right) + \frac{\kappa_{1,3}}{\kappa_{1,2} + \kappa_{1,3}} \frac{\kappa_{7,9}}{\kappa_{7,8} + \kappa_{7,9}} \left(\frac{1}{\kappa_{1,2} + \kappa_{1,3}} + \frac{1}{\kappa_{3,5}} + \frac{1}{\kappa_{5,6}} + \frac{1}{\kappa_{6,7}} + \frac{1}{\kappa_{7,8} + \kappa_{7,9}} + \frac{1}{\kappa_{9,10}} + \frac{1}{\kappa_{10,1}} \right) \right\}^{-1} \tag{A9}$$

Transition 7 ↔ 1 in Figure 3C. Similar to Equation (A2), the net transition flux $J_{7,1}^N$ can be expressed as,

$$J_{7,1}^N = \left(\frac{1}{\kappa_{1,2} + \kappa_{1,3}} + \frac{1}{\kappa_{2,4} + \frac{p_3}{p_2} (\kappa_{3,5} + \kappa_{3,6})} + \frac{1}{\kappa_{4,7} + \frac{p_5}{p_4} \kappa_{5,7} + \frac{p_6}{p_4} \kappa_{6,7}} + \frac{1}{\frac{p_4}{p_5} \kappa_{4,7} + \kappa_{5,7} + \frac{p_6}{p_5} \kappa_{6,7}} + \frac{1}{\frac{p_4}{p_6} \kappa_{4,7} + \frac{p_5}{p_6} \kappa_{5,7} + \kappa_{6,7}} + \frac{1}{\kappa_{7,1}} \right)^{-1} \tag{A10}$$

Application of Equations (15) and (16) to states 2, 3, 4, 5, and 6 (Figure 3C) generates the ratios of $p_2/p_3 = (\kappa_{1,2}(\kappa_{3,5} + \kappa_{3,6})) / (\kappa_{1,3}\kappa_{2,4})$, $p_4/p_5 = (\kappa_{1,2}(\kappa_{3,5} + \kappa_{3,6})\kappa_{5,7}) / (\kappa_{1,3}\kappa_{4,7}\kappa_{3,5})$, $p_5/p_6 = (\kappa_{3,5}\kappa_{6,7}) / (\kappa_{3,6}\kappa_{5,7})$, and $p_4/p_6 = (\kappa_{1,2}(\kappa_{3,5} + \kappa_{3,6})\kappa_{6,7}) / (\kappa_{1,3}\kappa_{4,7}\kappa_{3,6})$. Equation (A10) is simplified by replacing the ratios, namely,

$$J_{7,1}^N = \left\{ \frac{\kappa_{1,2}}{\kappa_{1,2} + \kappa_{1,3}} \left(\frac{1}{\kappa_{1,2} + \kappa_{1,3}} + \frac{1}{\kappa_{2,4}} + \frac{1}{\kappa_{4,7}} + \frac{1}{\kappa_{7,1}} \right) + \frac{\kappa_{1,3}}{\kappa_{1,2} + \kappa_{1,3}} \frac{\kappa_{3,5}}{\kappa_{3,5} + \kappa_{3,6}} \left(\frac{1}{\kappa_{1,2} + \kappa_{1,3}} + \frac{1}{\kappa_{3,5} + \kappa_{3,6}} + \frac{1}{\kappa_{5,7}} + \frac{1}{\kappa_{7,1}} \right) + \frac{\kappa_{1,3}}{\kappa_{1,2} + \kappa_{1,3}} \frac{\kappa_{3,6}}{\kappa_{3,5} + \kappa_{3,6}} \left(\frac{1}{\kappa_{1,2} + \kappa_{1,3}} + \frac{1}{\kappa_{3,5} + \kappa_{3,6}} + \frac{1}{\kappa_{6,7}} + \frac{1}{\kappa_{7,1}} \right) \right\}^{-1} \tag{A11}$$

Transition 5 ↔ 1 in Figure 3D. Similar to Equation (A2), the net transition flux $J_{5,1}^N$ can be expressed as,

$$J_{5,1}^N = \left(\frac{1}{\kappa_{1,2} + \kappa_{1,3}} + \frac{1}{\kappa_{2,5} + \frac{p_3}{p_2} \kappa_{3,4}} + \frac{1}{\frac{p_2}{p_3} \kappa_{2,5} + \kappa_{3,4}} + \frac{1}{\frac{p_4}{p_2} \kappa_{2,5} + \kappa_{4,5}} + \frac{1}{\kappa_{5,1}} \right)^{-1} \tag{A12}$$

Application of Equations (15) and (16) to states 2, 3, and 4 (Figure 3D) generates the ratios of $p_2/p_3 = (\kappa_{1,2}\kappa_{3,4})/(\kappa_{1,3}\kappa_{2,5})$ and $p_2/p_4 = (\kappa_{1,2}\kappa_{4,5})/(\kappa_{1,3}\kappa_{2,5})$. Equation (A12) is simplified by replacing the ratios, namely,

$$J_{5,1}^N = \left\{ \frac{\kappa_{1,2}}{\kappa_{1,2} + \kappa_{1,3}} \left(\frac{1}{\kappa_{1,2} + \kappa_{1,3}} + \frac{1}{\kappa_{2,5}} + \frac{1}{\kappa_{5,1}} \right) + \frac{\kappa_{1,3}}{\kappa_{1,2} + \kappa_{1,3}} \left(\frac{1}{\kappa_{1,2} + \kappa_{1,3}} + \frac{1}{\kappa_{3,4}} + \frac{1}{\kappa_{4,5}} + \frac{1}{\kappa_{5,1}} \right) \right\}^{-1} \tag{A13}$$

Transition 6 ↔ 1 in Figure 3E. Similar to Equation (A2), the net transition flux $J_{6,1}^N$ can be expressed as,

$$J_{6,1}^N = \left(\frac{1}{\kappa_{1,2} + \kappa_{1,3}} + \frac{1}{\kappa_{2,4} + \kappa_{2,5} + \frac{p_3}{p_2} \kappa_{3,5}} + \frac{1}{\frac{p_2}{p_3} (\kappa_{2,4} + \kappa_{2,5}) + \kappa_{3,5}} + \frac{1}{\kappa_{4,6} + \frac{p_5}{p_4} \kappa_{5,6}} + \frac{1}{\frac{p_4}{p_5} \kappa_{4,6} + \kappa_{5,6}} + \frac{1}{\kappa_{6,1}} \right)^{-1} \quad (\text{A14})$$

Applying Equations (15) and (16) to states 2, 3, 4, and 5 (Figure 3E) generates the ratios of $p_2/p_3 = (\kappa_{1,2}\kappa_{3,5})/(\kappa_{1,3}(\kappa_{2,4} + \kappa_{2,5}))$ and $p_4/p_5 = (\kappa_{1,2}\kappa_{2,4}\kappa_{5,6})/(\kappa_{4,6}(\kappa_{2,5}(\kappa_{1,2} + \kappa_{1,3}) + \kappa_{1,3}\kappa_{2,4}))$. Equation (A14) is simplified by replacing the ratios, namely,

$$J_{6,1}^N = \left\{ \frac{\kappa_{1,2}}{\kappa_{1,2} + \kappa_{1,3}} \frac{\kappa_{2,4}}{\kappa_{2,4} + \kappa_{2,5}} \left(\frac{1}{\kappa_{1,2} + \kappa_{1,3}} + \frac{1}{\kappa_{2,4} + \kappa_{2,5}} + \frac{1}{\kappa_{4,6}} + \frac{1}{\kappa_{6,1}} \right) + \frac{\kappa_{1,2}}{\kappa_{1,2} + \kappa_{1,3}} \frac{\kappa_{2,5}}{\kappa_{2,4} + \kappa_{2,5}} \left(\frac{1}{\kappa_{1,2} + \kappa_{1,3}} + \frac{1}{\kappa_{2,4} + \kappa_{2,5}} + \frac{1}{\kappa_{5,6}} + \frac{1}{\kappa_{6,1}} \right) + \frac{\kappa_{1,3}}{\kappa_{1,2} + \kappa_{1,3}} \left(\frac{1}{\kappa_{1,2} + \kappa_{1,3}} + \frac{1}{\kappa_{3,5}} + \frac{1}{\kappa_{5,6}} + \frac{1}{\kappa_{6,1}} \right) \right\}^{-1} \quad (\text{A15})$$

Appendix C. Actual Transition Rate and Ratio at Branching

The probability density of a stochastic transition occurring at time t satisfies the distribution of $p(t) = e^{-t/\tau}/\tau$, where τ is the average transition time, namely, $\tau = \int_0^\infty tp(t)dt$. If there are two transitions, for example $1 \rightarrow 2$ and $1 \rightarrow 3$, competing at a branching state (state 1), we can assume both the transitions satisfy the distribution above, and their original transition times in the absence of the branching are $\tau_{1,2}$ and $\tau_{1,3}$, respectively. In the presence of the branching, their actual transition times are changed by the branching. The branching probability for $1 \rightarrow 2$ is,

$$\rho_{1,2} = \int_0^\infty dt_{1,3} \frac{e^{-t_{1,3}/\tau_{1,3}}}{\tau_{1,3}} \int_0^{t_{1,3}} dt_{1,2} \frac{e^{-t_{1,2}/\tau_{1,2}}}{\tau_{1,2}} = \frac{1/\tau_{1,2}}{1/\tau_{1,2} + 1/\tau_{1,3}} \quad (\text{A16})$$

while the actual transition time for $1 \rightarrow 2$ is,

$$\tau'_{1,2} = \frac{1}{\rho_{1,2}} \int_0^\infty dt_{1,3} \frac{e^{-t_{1,3}/\tau_{1,3}}}{\tau_{1,3}} \int_0^{t_{1,3}} dt_{1,2} \frac{t_{1,2} e^{-t_{1,2}/\tau_{1,2}}}{\tau_{1,2}} = \frac{1}{1/\tau_{1,2} + 1/\tau_{1,3}} \quad (\text{A17})$$

Similarly, $\rho_{1,3} = (1/\tau_{1,3})/(1/\tau_{1,2} + 1/\tau_{1,3})$ and $\tau'_{1,3} = 1/(1/\tau_{1,2} + 1/\tau_{1,3})$. The results derived in the main text for Figures 2 and 3 are consistent with these results.

References

1. Meisl, G.; Kirkegaard, J.B.; Arosio, P.; Michaels, T.C.; Vendruscolo, M.; Dobson, C.M.; Linse, S.; Knowles, T.P. Molecular mechanisms of protein aggregation from global fitting of kinetic models. *Nat. Protoc.* **2016**, *11*, 252–272. [[CrossRef](#)] [[PubMed](#)]
2. Perez-Hernandez, G.; Paul, F.; Giorgino, T.; De Fabritiis, G.; Noé, F. Identification of slow molecular order parameters for markov model construction. *J. Chem. Phys.* **2013**, *139*, 015102. [[CrossRef](#)] [[PubMed](#)]
3. Bertaglia, G.; Pareschi, L. Hyperbolic models for the spread of epidemics on networks: Kinetic description and numerical methods. *ESAIM-Math. Model. Numer. Anal. -Model. Math. Anal. Numer.* **2021**, *55*, 381–407. [[CrossRef](#)]
4. Ajmone Marsan, G.; Bellomo, N.; Gibelli, L. Stochastic evolutionary differential games toward a systems theory of behavioral social dynamics. *Math. Models Methods Appl. Sci.* **2016**, *26*, 1051–1093. [[CrossRef](#)]
5. Hill, T.L.; Chen, Y.D. Stochastics of cycle completions (fluxes) in biochemical kinetic diagrams. *Proc. Natl. Acad. Sci. USA* **1975**, *72*, 1291–1295. [[CrossRef](#)]
6. Hill, T.L. Discrete-time random walks on diagrams (graphs) with cycles. *Proc. Natl. Acad. Sci. USA* **1988**, *85*, 5345–5349. [[CrossRef](#)]
7. Liepelt, S.; Lipowsky, R. Kinesin's network of chemomechanical motor cycles. *Phys. Rev. Lett.* **2007**, *98*, 258102. [[CrossRef](#)]
8. Lipowsky, R.; Liepelt, S. Chemomechanical coupling of molecular motors: Thermodynamics, network representations, and balance conditions. *J. Stat. Phys.* **2008**, *130*, 39–67. [[CrossRef](#)]
9. Cao, J.; Silbey, R.J. Generic schemes for single-molecule kinetics. 1: Self-consistent pathway solutions for renewal processes. *J. Phys. Chem. B* **2008**, *112*, 12867–12880. [[CrossRef](#)]
10. Chaudhury, S.; Cao, J.; Sinityn, N.A. Universality of poisson indicator and fano factor of transport event statistics in ion channels and enzyme kinetics. *J. Phys. Chem. B* **2013**, *117*, 503–509. [[CrossRef](#)]
11. Cao, J. Michaelis-menten equation and detailed balance in enzymatic networks. *J. Phys. Chem. B* **2011**, *115*, 5493–5498. [[CrossRef](#)] [[PubMed](#)]
12. Ren, J. Detectable states, cycle fluxes, and motility scaling of molecular motor kinesin: An integrative kinetic graph theory analysis. *Front. Phys.* **2017**, *12*, 120505. [[CrossRef](#)]

13. Li, X.; Kolomeisky, A.B. Mechanisms and topology determination of complex chemical and biological network systems from first-passage theoretical approach. *J. Chem. Phys.* **2013**, *139*, 144106. [[CrossRef](#)] [[PubMed](#)]
14. Mugnai, M.L.; Hyeon, C.; Hinczewski, M.; Thirumalai, D. Theoretical perspectives on biological machines. *Rev. Mod. Phys.* **2020**, *92*, 025001. [[CrossRef](#)]
15. Qian, H.; Bishop, L.M. The chemical master equation approach to nonequilibrium steady-state of open biochemical systems: Linear single-molecule enzyme kinetics and nonlinear biochemical reaction networks. *Int. J. Mol. Sci.* **2010**, *11*, 3472–3500. [[CrossRef](#)]
16. Nishiyama, M.; Higuchi, H.; Yanagida, T. Chemomechanical coupling of the forward and backward steps of single kinesin molecules. *Nat. Cell Biol.* **2002**, *4*, 790–797. [[CrossRef](#)]
17. Carter, N.J.; Cross, R.A. Mechanics of the kinesin step. *Nature* **2005**, *435*, 308–312. [[CrossRef](#)]
18. Clancy, B.E.; Behnke-Parks, W.M.; Andreasson, J.O.L.; Rosenfeld, S.S.; Block, S.M. A universal pathway for kinesin stepping. *Nat. Struct. Mol. Biol.* **2011**, *18*, 1020–1027. [[CrossRef](#)]
19. Yasuda, R.; Noji, H.; Kinosita, K., Jr.; Yoshida, M. F-1-atpase is a highly efficient molecular motor that rotates with discrete 120 degrees steps. *Cell* **1998**, *93*, 1117–1124. [[CrossRef](#)]
20. Toyabe, S.; Watanabe-Nakayama, T.; Okamoto, T.; Kudo, S.; Muneyuki, E. Thermodynamic efficiency and mechanochemical coupling of f-1-atpase. *Proc. Natl. Acad. Sci. USA* **2011**, *108*, 17951–17956. [[CrossRef](#)]
21. Soga, N.; Kimura, K.; Kinosita, K., Jr.; Yoshida, M.; Suzuki, T. Perfect chemomechanical coupling of fof1-atp synthase. *Proc. Natl. Acad. Sci. USA* **2017**, *114*, 4960–4965. [[CrossRef](#)] [[PubMed](#)]
22. Petersen, J.; Forster, K.; Turina, P.; Gräber, P. Comparison of the h+/atp ratios of the h+-atp synthases from yeast and from chloroplast. *Proc. Natl. Acad. Sci. USA* **2012**, *109*, 11150–11155. [[CrossRef](#)] [[PubMed](#)]
23. Schnakenberg, J. Network theory of microscopic and macroscopic behavior of master equation systems. *Rev. Mod. Phys.* **1976**, *48*, 571–585. [[CrossRef](#)]
24. Seifert, U. Entropy production along a stochastic trajectory and an integral fluctuation theorem. *Phys. Rev. Lett.* **2005**, *95*, 040602. [[CrossRef](#)]
25. Hou, R.; Wang, Z. Thermodynamic marking of fof1 atp synthase. *Biochim. Biophys. Acta-Bioenerg.* **2021**, *1862*, 148369. [[CrossRef](#)] [[PubMed](#)]
26. Qian, H.; Kjelstrup, S.; Kolomeisky, A.B.; Bedeaux, D. Entropy production in mesoscopic stochastic thermodynamics: Nonequilibrium kinetic cycles driven by chemical potentials, temperatures, and mechanical forces. *J. Phys. Condens. Matter* **2016**, *28*, 153004. [[CrossRef](#)] [[PubMed](#)]
27. Hatano, T.; Sasa, S. Steady-state thermodynamics of langevin systems. *Phys. Rev. Lett.* **2001**, *86*, 3463–3466. [[CrossRef](#)] [[PubMed](#)]
28. Oono, Y.; Paniconi, M. Steady state thermodynamics. *Prog. Theor. Phys. Suppl.* **1998**, *130*, 29–44.
29. Ge, H. Extended forms of the second law for general time-dependent stochastic processes. *Phys. Rev. E* **2009**, *80*, 021137. [[CrossRef](#)]
30. Seifert, U. Stochastic thermodynamics, fluctuation theorems and molecular machines. *Rep. Prog. Phys.* **2012**, *75*, 126001. [[CrossRef](#)]
31. Landi, G.T.; Paternostro, M. Irreversible entropy production: From classical to quantum. *Rev. Mod. Phys.* **2021**, *93*, 035008. [[CrossRef](#)]
32. Wang, Z.; Hou, R.; Efremov, A. Directional fidelity of nanoscale motors and particles is limited by the 2nd law of thermodynamics via a universal equality. *J. Chem. Phys.* **2013**, *139*, 035105. [[CrossRef](#)] [[PubMed](#)]
33. Hou, R.; Wang, Z. Role of directional fidelity in multiple aspects of extreme performance of the f-1-atpase motor. *Phys. Rev. E* **2013**, *88*, 252–272. [[CrossRef](#)] [[PubMed](#)]
34. Meisl, G.; Kirkegaard, J.B.; Arosio, P.; Michaels, T.C.; Vendruscolo, M.; Dobson, C.M.; Linse, S.; Knowles, T.P. Autonomous synergic control of nanomotors. *ACS Nano* **2014**, *8*, 1792–1803.
35. Hou, R.; Loh, I.Y.; Li, H.; Wang, Z. Mechanical-kinetic modeling of a molecular walker from a modular design principle. *Phys. Rev. Appl.* **2017**, *7*, 024020. [[CrossRef](#)]